AJNR Am J Neuroradiol 23:1524–1532, October 2002

Reproducibility of Primary Motor Cortex Somatotopy Under Controlled Conditions

Hatem Alkadhi, Gerard R. Crelier, Sabina Hotz Boendermaker, Xavier Golay, Marie-Claude Hepp-Reymond, and Spyros S. Kollias

BACKGROUND AND PURPOSE: **The somatotopic organization of the contralateral primary motor cortex (M1) and its intra- and intersubject reproducibility has been the subject of many investigations and controversies. A potential explanation for a least some of the conflicting results could be the lack of movement control in the studies performed. The purpose of this study was to investigate these issues under controlled experimental conditions.**

METHODS: **Functional MR imaging was performed in 12 healthy volunteers performing hand, finger, wrist, elbow, foot, and tongue movements. Two experimental sessions were separated by 2 weeks. Controlled conditions were achieved by means of a custom-designed arm and hand manipulandum providing standardization of the movements within and across subjects.**

RESULTS: **The experiments revealed a clear large-scale somatotopy of the contralateral M1 with distinct subregions controlling the foot, arm, and tongue. Despite considerable overlap of the volumes, geometric centers of gravity (COGs) showed statistically significant differences in coordinates between the elbow, wrist, fingers, and hand. COGs showed a high degree of intra- and interindividual reproducibility, particularly for the upper limb movements, in contrast to the activation volumes that proved to be unreliable parameters, despite the controlled conditions.**

CONCLUSION: **These findings support the existence of a gross-scale somatotopic organization yet also demonstrate a clear, fine-scale somatotopy of the within-arm representations. Furthermore, they reveal high reproducibility of the COGs when standardized conditions are applied. This observation highlights the need for movement control to allow for intra- and intersubject comparison.**

The debate over whether various body parts in humans and nonhuman primates activate topographically separate subregions in the contralateral primary motor cortex (M1) in a somatotopic fashion has continued since Jackson's original observations in patients with focal epilepsy (1). The results of Foerster's electrical stimulation studies (2) confirmed these fundamental findings and were subsequently extended by Penfield and Boldrey (3), who mapped the entire sensorimotor cortex. However, the existence of a simple and regularly organized somatotopy, particularly in its fine scale, has been questioned with the application of intracortical microstimulation in nonhuman primates that yield improved spatial resolution (4, 5). Findings from recent microstimulation and lesion studies also suggest the presence of highly distributed networks in which movements and muscles are intermingled without an evident somatotopy as the main organizing principle (6, 7). By using noninvasive methods, recent investigations of human M1 hand and finger representations have had conflicting results concerning both the distributed organization and the original somatotopic arrangement. For example, Sanes and collaborators (8) found a major spatial overlap with no evidence for somatotopy of the finger and wrist movements by using functional MR (fMR) imaging. Moreover, magnetencephalography reveals separable neuronal sources for wrist and finger movements, though in a nonsomatotopic fashion (9). In contrast, findings from a recent analysis involving contrasting finger movements as the control tasks suggest the existence of a discrete somatotopic gradient for finger movements in the presence of notable overlap (10).

A common observation in many brain imaging investigations is the considerable variability in the loca-

Received November 11, 2001; accepted May 28, 2002.

From the Institute of Neuroradiology, University Hospital Zurich (H.A., G.R.C., X.G., S.S.K.), and the Institute of Neuroinformatics, University and ETH Zurich (S.H.B., M.-C.H.-R.), Switzerland.

Supported by the Swiss National Research Program NRP 38 #4038–052837/1 and by the NCCR on Neural Plasticity and Repair.

Presented at the Annual Meeting of the American Society of Neuroradiology in Boston, MA, 2001.

Address reprint requests to Spyros S. Kollias, MD, Institute of Neuroradiology, University Hospital Zurich, Frauenklinikstrasse 10, CH-8091 Zurich, Switzerland.

tion of body parts in M1 and in the extent of activation (9–15). Most of these studies required the performance of nonstandardized movements and thus may have been inappropriate for the evaluation of intra- and interindividual variations in somatotopy. The uncontrolled movements could easily account for the frequent variability (14). In addition, the consistency and reproducibility of M1 activation patterns over time are rarely investigated, both within groups and within individuals (11, 13, 15, 16). However, basic data on test-retest reliability must be established, and we must be able to reliably distinguish differences in activation over time as real changes rather than changes due to methodological problems or individual biologic variations.

By using high-spatial-resolution functional fMR imaging, we aimed to systematically re-examine the aforementioned issues. The specific questions addressed were the following: 1) the topographic representation of the various body parts, including the within-arm somatotopy in contralateral M1 and its interindividual variability, and 2) the reproducibility of the fMR imaging data within and across subjects. To specifically address the issue of controlled movement execution, we designed a particular arm and hand support to standardize upper limb movements across all subjects. We hypothesized that the functional M1 organization concurrently reflects both the somatotopy and the distributed overlap of the various body part representations. Furthermore, we wanted to determine if the controlled experimental conditions yield highly reproducible intra- and interindividual activation patterns.

Methods

Subjects

Twelve healthy subjects (six female, six male; mean age, 29.9 years ± 4.1; age range, 25–39 years) without any history of neurologic or psychiatric illness were recruited for this study. Hand dominance was determined according to the Chapman and Chapman handedness inventory (17). The subjects had an explicit right hand dominance, with a mean inventory scale score of 13.2. Subjects provided written informed consent before undergoing MR imaging, and our institutional review board approved the experimental protocol.

Imaging Procedures

Imaging was performed by using a 1.5-T whole-body machine (Signa Horizon; Echo-speed LX GE Medical Systems, Milwaukee, WI) equipped with a standard product transmit-receive head coil. Foam pads and restraining strips were used to restrict the patient's head motion in the coil. T1-weighted whole-brain anatomic reference-volume data sets were acquired with an isotropic spatial resolution of 1.2 mm by using a three-dimensional spoiled gradient-echo sequence (TR/TE, 50/9; flip angle, 45°). Functional imaging was conducted by using a gradient-echo echo-planar pulse sequence (3750/40 ms; flip angle, 90°) that was sensitive to the blood oxygen level–dependent (BOLD) signal intensity. We acquired 30 contiguous axial 4-mm-thick sections to cover the entire brain. The imaging matrix consisted of 128 × 96 data points, resulting in a rectangular field of view of 256 ×192 mm and a nominal in-plane resolution of 2 × 2 mm. Series of 48 sequential volumes were acquired for each functional experiment. Simulations with computer-generated signals previously confirmed that, with 48 measured time points, more than 98.5% of the correlated pixels with a signal intensity change of 1% are detected (18). Pixels with a signal intensity change of more than 1% are detected almost 100% of the time. Keeping the fMR imaging experiments brief allowed us to limit the imaging time to 45 minutes, which was well tolerated by all subjects. (The imaging time becomes an important issue when extending these investigations to patients.)

Activation Paradigms and Manipulandum

All subjects underwent the entire imaging protocol twice. The follow-up session occurred within 14 days of the initial session. Each activation experiment consisted of three 30-second periods of rest alternating with three 30-second periods of movement. The duration of the total data collection was 180 seconds. The beginning and end of each motor activation period was signaled with start and stop instructions that were verbally transmitted over the machine's intercom system. All subjects received written information about the experimental protocol and instructions the day before data acquisition. To ensure a proper task execution, each movement was practiced first outside and then inside the magnet bore before imaging. During data acquisition, the examiner (H.A.) monitored the subject and controlled the performance by watching for any movement or apparent change in the resting state of the nonmoving limbs. Assessment of surface electromyography during the fMR imaging experiments usually lacks the sensitivity to depict small, undesired movements due to gradient-induced artifacts. It can only be performed by using a specific registration system and experimental protocol (19), and it was not performed in this study.

Six series of self-paced movements were performed at a rate of approximately 0.5 Hz in the following order: 1) repetitive flexion (40°) and extension (20°) of the right wrist; 2) flexion (100°) and extension (−30°) of the right elbow; 3) opening and closing of all fingers of the right hand with the wrist fixed in a slight extension (15°, natural resting position of the hand); 4) repetitive, sequential finger to thumb opposition of the right digits 2–5; 5) plantar (45°) and dorsal flexion (10°) of the right foot at the ankle; and 6) bilateral horizontal movements of the tongue.

To standardize the movements and thus allow for inter- and intrasubject comparisons, an adaptable glass-fiber forearm splint was designed. This splint was mounted at the height of the elbow on a rotational axis fixed onto the imaging table. The split kept the forearm in a comfortable, slightly flexed position over the subject's abdomen at an angle of approximately 35° relative to the imaging table. The movements of the wrist, hand, and fingers were restrained by applying strips and cast elements between the experiments, without repositioning of the subject. During the movements of a specific joint, potential movements of the other joints were prevented by using additional devices and strips (eg, wrist and fingers were restrained during elbow movements). The movements of the tongue and the right foot were unconstrained. The left arm was positioned along the patient's body, and the lateral wall of the magnet bore and additional strips restricted unintentional movements. During the experiments, the subjects closed their eyes, and the light in the imaging room was dimmed.

Analysis of fMR Imaging Data

All data analysis and postprocessing was performed off-line. To minimize artifacts due to residual head motion, functional volumes were realigned for each experiment by using a rigid-body registration algorithm (20). In accordance with the method Hopfinger et al recently used (21), the data were spatially filtered by using a three-dimensional Gaussian convolution kernel of 4 mm at full width half maximum. Because the spatial extent of cortical activation was expected to be in the

order of 3–5 mm, an optimal smoothing kernel of 4 mm was chosen to increase the sensitivity of our analysis and, at the same time, to maintain the high nominal spatial resolution of our raw data ($2 \times 2 \times 4$ mm) as much as possible.

By using a fully automated procedure, anatomic reference volumes were registered to the Montreal average volumetric data set aligned on the Talairach stereotactic coordinate system (22). The resulting transformation was then used to resample the functional data into stereotactic space. The functional data were postprocessed by using an improved cross-correlation analysis (23). Voxels activated during the task conditions were identified by calculating nonparametric Spearman rank-order correlation coefficients between the time series of pixel intensities and an idealized response function with a time shift of 4 seconds to account for the hemodynamic delay. Transformations to the Student *t* statistics were made (24); only pixels with a statistically significant correlation ($P < .001$, not corrected for multiple comparisons) were considered as activated areas.

For the group analysis, a statistical analysis based on a linear model with correlated errors was performed for each data set (25). The design matrix of the linear model was first convolved with a gamma hemodynamic response function, as Glover proposed (26). Drift was removed by adding polynomial covariates in the frame times, up to degree 3, to the design matrix. In a second step, experiments were combined by using a fixed effect analysis also based on a linear model (27). Thresholds for thee resulting *t* statistic images were set by using the minimum given by a combination of Bonferroni correction and random field theory (25). This statistical test was performed for each individual task.

Quantitative and Statistical Analysis of Activated Regions

To evaluate activation in the contralateral M1, a trained neuroradiologist (H.A.) separately segmented each anatomic reference volume a priori, purely on the basis of structural anatomy, before the functional data were analyzed. M1 was anatomically defined as the cortex lying within the posterior bank of the precentral gyrus, including the central sulcus and extending to the paracentral lobule. Although the exact anterior border of M1 cannot be defined on the basis of only macroscopic landmarks (28), we defined M1 as spanning over the posterior two-thirds of the precentral gyrus.

These segmented regions were used as regions of interest for the quantitative analysis of activated areas. Spatially contiguous activated voxels inside these regions were unified into individual clusters. Voxels that did not belong to a cluster of at least three voxels above the significance threshold were eliminated on the assumption that small isolated activation patches are likely to be artifactual. For each cluster, the volume of activation, the maximum signal intensity (maximum *t* value), and the geometric center of gravity (COG) were determined and their location in Talairach coordinates retained. For the COG calculation, homogeneous mass distribution in each cluster was assumed, and therefore, all voxels above the significance threshold were uniformly weighted. The COG calculation was preferred to activation maximum analysis, because COGs are less sensitive to random fluctuations and local signal intensity to noise variations and because they better represent shifts in extended activations (14, 29). Furthermore, activation maxima are highly variable and relatively dependent on evaluator-specific interpretations (14).

The normal distribution of the volumes of activation and COG locations across experiments and across subjects was statistically assessed by means of Kolmogorov-Smirnov tests. Potential differences in the localization of COGs (in the anteroposterior, lateral-medial, and cranial-caudal directions) and activated volumes for movements of various body parts within sessions were statistically tested by using paired *t* tests. The degree of overlap between different body part representations within sessions was calculated by relating the overlapping volume to the totally activated volume resulting from the two movements, with the overlaps counted only once. This type of overlapping volume calculation was intended to restrict nonspecific activation as much as possible (29). The reproducibility of the localization of the COGs and activated volumes across sessions was also assessed by using paired *t* tests. To further estimate the degree of reproducibility of the coordinates across sessions, the means and SDs of all three-dimensional distances within subjects were calculated by using the formula of Pythagoras.

Results

In a total of 24 sessions with six movement series each, 144 functional imaging experiments were performed. Results of two experiments with foot movements and two with tongue movements were discarded because of uncorrectable motion artifacts.

Cortical and Subcortical Areas Activated by Simple Movements

Activation was detected in the contra- and ipsilateral M1 and in nonprimary motor, parietal, and subcortical areas during all movements (Fig 1 and 2). The nonprimary motor areas were referred to as the dorsal and ventral premotor cortex and the supplementary and cingulate motor areas (12). Subcortical activation occurred in the basal ganglia, thalamus, and cerebellum. Ipsilateral M1, basal ganglia, and thalamic activation was inconstant and occurred in only some experiments and individuals, whereas the other cortical and cerebellar areas were consistently active during all movements tested. A further analysis of these areas was not undertaken in the present study, which explicitly focused on contralateral M1 and the reproducibility of its activation.

Somatotopic Organization of the Contralateral Primary Motor Cortex

Statistically significant MR signal intensity changes were observed within contralateral M1 in all subjects and for all movements. To assess the topographic organization within M1, we report findings from both the single-subject and group analyses. For the group analysis, the data acquired in both sessions were computed, yielding 24 acquisition sessions per movement type (12 subjects, two sessions).

The volumes of activation in the contralateral M1 varied considerably between subjects (mean for all movements, 3161 $mm^3 \pm 1555$; range, 256–9600 mm^3), despite the controlled experimental conditions. Statistically significant differences ($P < .0001$) in activated volumes were present only for the hand movement. As compared with the sequential finger to thumb opposition, the finger movements activated a volume (2997 $mm^3 \pm 1208$) smaller than that activated by opening and closing the hand (5284 $mm^3 \pm 1952$), which required synchronous flexion and extension of all fingers (Table 1). In contrast, the maximum *t* values were constant (mean, 9.9 ± 1.5) across all subjects and movement types (Table 1).

Cortical maps acquired during the execution of all

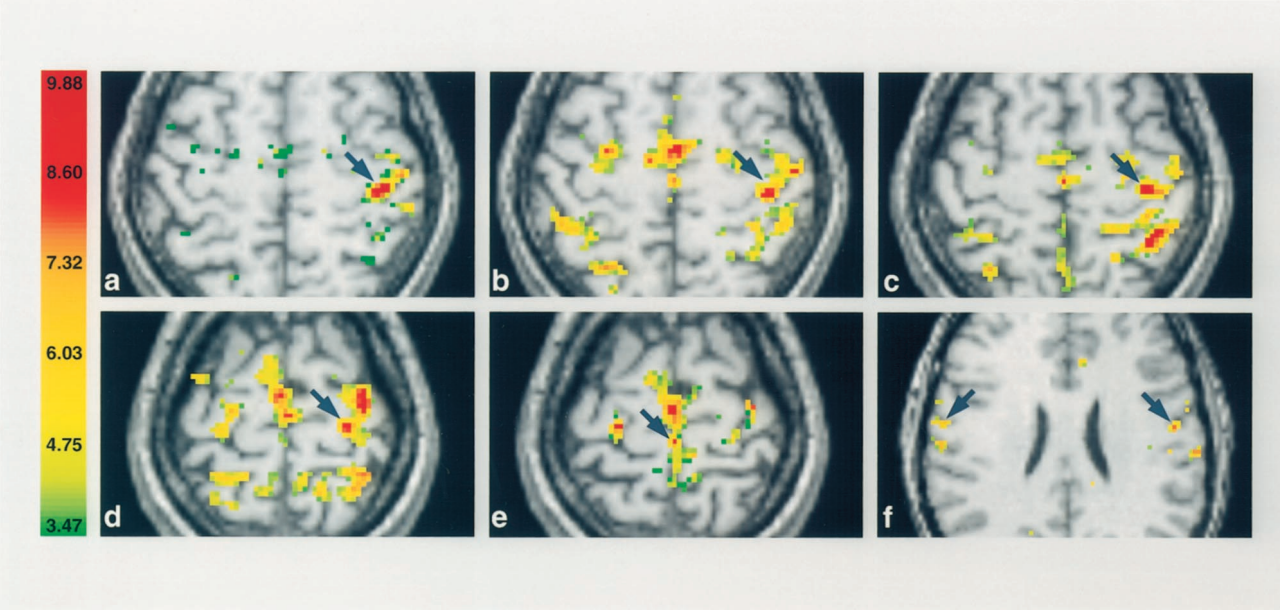

FIG 1. Activation in contralateral M1 (*arrows*) displayed in axial sections for one subject in the first session. The right side of the sections corresponds to the left hemisphere, and the numbers in the color bar correspond to *t* values.

A and *B*, The fingers (*A*) and hand (*B*) are in almost identical locations (*z* plane, +58).

C and *D*, The wrist (*C*) and elbow (*D*) representations are located more medially, superior and posterior along the course of M1 (*z* plane, +59 and +61, respectively).

E and *F*, Note the considerable overlap of activated volumes within the arm and the clear separation of the foot (*E*) and tongue (*F*) (*z* plane, +66 and +28, respectively).

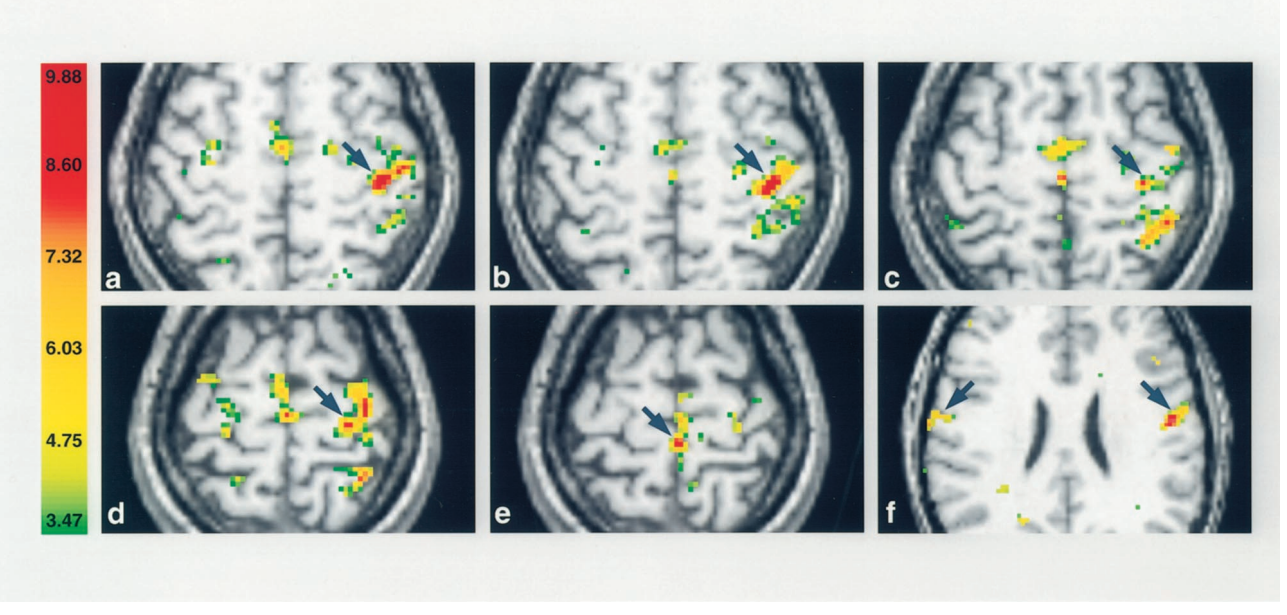

FIG 2. Activation of contralateral M1 in the second session in the same subject as in Figure 1. A comparison with the images in Figure 1 reveals a high degree of reproducibility in the somatotopy despite variations in the activated volumes.

A and *B*, Fingers (*A*) and hand (*B*).

C and *D*, Wrist (*C*) and elbow (*D*).

E and *F*, Foot (*E*) and tongue (*F*).

six movements in one representative subject are shown in Figure 1. The considerable overlap of activated volumes for the forearm movements (fingers, hand, wrist, and elbow) can be seen. Quantitative single-subject analysis in all individuals and in both sessions revealed a mean percentage volume overlap ranging from 14% for the fingers with the elbow to 86% for the fingers with hand opening and closing (Table 2).

Both single-subject and group analyses showed that the averaged COGs occurred in a somatotopic order within M1, with the wrist and elbow being more medial, posterior, and superior along the course of M1, compared with the hand and finger representations

TABLE 1: Activation in contralateral M1 areas of body parts

Paradigm	Volume of Contralateral M1, mm³		Maximum *t* Value*	COG		
	Mean ± SD	Range		x	y	z
Hand	5566 ± 2473	2976–9600	9.7 ± 2.0	−36 ± 3	−22 ± 4	58 ± 3
Fingers	2972 ± 1211	1264–5129	8.4 ± 2.6	−37 ± 2	−20 ± 5	58 ± 2
Wrist	4409 ± 2091	1520–8320	9.4 ± 2.4	−34 ± 3	−23 ± 4	59 ± 3
Elbow	2267 ± 1158	1200–7824	8.2 ± 2.3	−29 ± 4	−25 ± 4	61 ± 5
Foot	1457 ± 986	256–3888	5.9 ± 1.2	−6 ± 3	−33 ± 5	66 ± 5
Tongue†						
Left	3079 ± 2034	1088–7152	7.9 ± 1.5	−52 ± 3	−5 ± 3	29 ± 6
Right	3042 ± 164	512–6272	7.3 ± 1.7	56 ± 2	−6 ± 3	28 ± 5

Note.—Data are from the single-subject analysis. Numbers of subjects were as follows: 24 for the hand, fingers, wrist, and elbow experiments and 22 for the tongue and foot experiments.

* Data are the mean ± SD.

† For the tongue movements, the bilateral representations in the left and right hemispheres are shown.

TABLE 2: Statistical comparisons

Comparison	*P* Value from *t* Test			Mean Overlapping Volume, %*
	x	y	z	
Hand versus wrist	<.001	<.07	<.001	49% ± 14
Hand versus elbow	<.001	<.001	<.001	28% ± 16
Finger versus hand	>.05	>.05	>.05	86% ± 10
Finger versus wrist	<.001	<.001	<.001	34% ± 14
Finger versus elbow	<.001	<.001	<.001	14% ± 10
Wrist versus elbow	<.001	<.001	<.001	32% ± 14

Note.—Comparisons of the COGs and the percentage of overlapping volumes for the finger, hand, wrist, and elbow movements in contralateral M1. Data are from the single-subject analysis. Numbers of subjects were as follows: 24 for the hand, fingers, wrist, and elbow experiments and 22 for the tongue and foot experiments.

* Data are the mean ∀ SD.

(Table 1). The mean COGs for hand opening and closing and for the sequential finger to thumb opposition were in almost identical locations. Within the forearm, statistically significant differences were found between the COGs of the hand and elbow, wrist and elbow, individual fingers and wrist, and individual fingers and elbow for all three coordinates ($P < .001$) (Table 2). Significant differences were also detected between hand and wrist movements for the *x* and *z* coordinates but not for the *y* coordinate ($P < .07$) (Table 2). The coordinates for finger to thumb opposition and for hand movements did not differ significantly. As expected, the averaged COGs of the foot and left hemispheric tongue representation were spatially separated ($P < .001$) and did not overlap with the forearm M1 representations (Fig 1, Table 1).

Figure 3 displays the axial and coronal two-dimensional scatter plots and the COG projections for the six movements and for the 12 subjects in both sessions. The figure illustrates the clearly separate M1 subdivisions of the foot—which are most medial, posterior (axial), and superior (coronal)—and the M1 subdivisions the tongue—which are lateral, anterior (axial), and inferior (coronal). Those for the arm are in between. Within the arm representation, the local distribution of the mean COGs of the elbow, wrist, fingers, and hand shows a clear somatotopic gradient. In this figure, the overlap of the COGs for some within-arm movements in some subjects with the COGs of adjacent joints in other individuals was obvious. This partly overlapping distribution of interindividual COGs was due to anatomic variability between subjects. However, the somatotopic gradient in each subject was preserved. This finding can be appreciated in Figure 4A, which displays the axial two-dimensional scatter plots of the COGs of the fingers, hand, wrist, and elbow in the contralateral M1 in the first experiment of each subject.

Reproducibility of the Somatotopic Organization

When the volumes of activation of both imaging sessions were compared within subjects, considerable variations were revealed for each movement within the contralateral M1, as can be seen in the means and SDs listed in Table 3. The paired *t* tests revealed that these variations in volume were not significantly different across sessions. Figure 2 displays the cortical maps obtained for the six movement types during the second session in the same subject as in Figure 1. The intraindividual variability in the extent of the activated volumes (when compared with the findings in Fig 1) is obvious.

The reproducibility of the anatomic location was addressed by using paired *t* tests to compare the COG coordinates for each movement in the first and second imaging sessions. For this analysis, the data acquired in each session were computed separately to yield two 12-acquisition sessions per movement type (12 subjects per session). As can be seen in Table 3, the coordinates of many COGs were identical in both sessions. The measured differences were only in the 1-mm range (rarely were they 2 mm), except for the *z* coordinate of the bilateral tongue representations. The statistical comparison of the data from the first and second experimental sessions did not reveal any significant difference in all three coordinates for any of movements.

When we compared the intraindividual mean three-dimensional distance between the COGs in the first and second imaging sessions, the smallest distances were found for the wrist (2 mm ± 1), foot

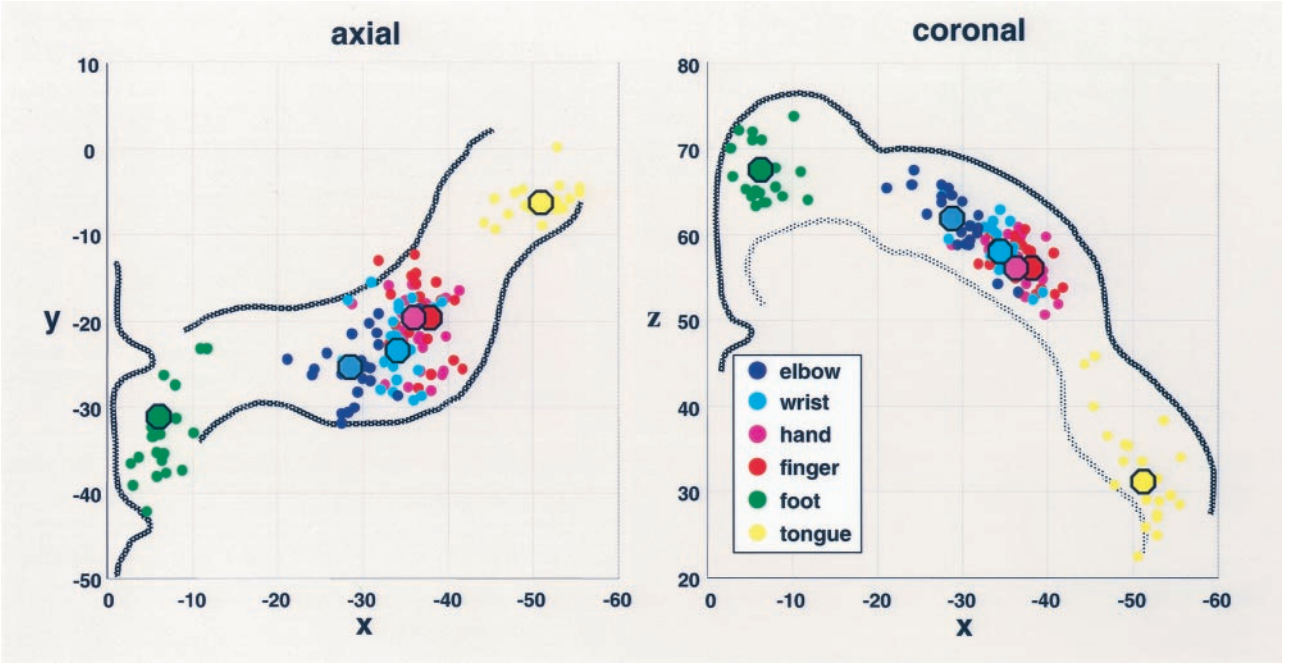

FIG 3. Two-dimensional scatter plots of the COGs in the 12 subjects (two sessions per subject) in the contralateral M1. *Small dots* represent individual COGs, and *large dots* indicate the mean COGs. Note the separate subdivisions for the foot, arm, and tongue and the clear somatotopic gradients within the arm representations in both the axial and coronal planes. The *x*, *y*, and *z* coordinates corresponding to those in Talairach space (21). *Left,* Axial plane with approximate contour of the precentral gyrus. *Right,* Coronal plane with the cortical surface and limited to the white matter.

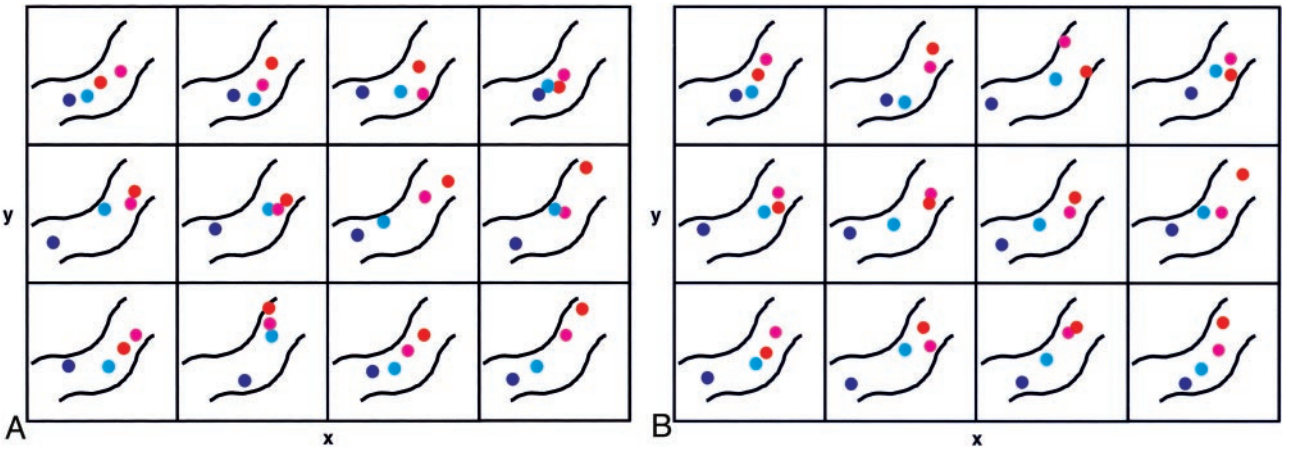

FIG 4. Two-dimensional scatter plots of within-forearm COGs in contralateral M1 in the 12 subjects. COGs plane for the fingers, hand, wrist, and elbow are displayed in the axial plane.

A, First experimental session. The approximate contour of the precentral gyrus is outlined (as in Fig 3 *left* image, with the same colors as in Fig 3). The width *x* of each rectangle is 20 mm and the height *y* is 18 mm in Talairach space. Note the preserved somatotopic gradient in all 12 individual hand and forearm representations.

B, Second experimental session. Note the highly similar distribution and preserved somatotopic gradient of within-forearm COGs in almost all subjects compared with those of first session.

(2 mm ± 2), hand (3 mm ± 2), finger (4 mm ± 2), and elbow (4 mm ± 3) movements. This observation is demonstrated in Figure 4B, which displays the axial two-dimensional scatter plots of the COGs in the second experiment for all within-arm movements in each subject. Compared with Figure 4A, the high reproducibility and similar distributions of the COGs in almost all individuals across both sessions can be estimated. The largest variability in COGs was found with the left (4 mm ± 2) and right hemispheric (7 mm ± 4) tongue representations and was most probably related to the difficulty in performing this unrestricted movement in a controlled and regular manner.

Discussion

The main findings of this study can be summarized as follows (1). Earlier data on a clear large-scale somatotopic organization of the contralateral M1 with distinct subregions controlling movements of the foot, arm, and face are confirmed (2). Statistically

TABLE 3: Reproducibility of the COGs and activated volumes in contralateral M1

Experiment and Session	Mean Volume	x	y	z
Fingers				
First	2972 ± 1211	−37 ± 2	−20 ± 5	58 ± 2
Second	3023 ± 1263	−37 ± 3	−19 ± 4	57 ± 3
Wrist				
First	4409 ± 2091	−34 ± 3	−23 ± 4	59 ± 3
Second	3519 ± 1760	−34 ± 3	−22 ± 5	59 ± 3
Elbow				
First	2267 ± 1158	−29 ± 4	−25 ± 4	61 ± 5
Second	1984 ± 453	−29 ± 2	−26 ± 3	62 ± 3
Hand				
First	5566 ± 2473	−36 ± 3	−22 ± 4	58 ± 3
Second	5002 ± 1309	−37 ± 2	−20 ± 4	57 ± 3
Foot				
First	1457 ± 986	−6 ± 3	−33 ± 5	66 ± 5
Second	1436 ± 955	−6 ± 3	−33 ± 5	68 ± 4
Tongue, Left				
First	3079 ± 2034	−52 ± 3	−5 ± 3	29 ± 6
Second	3907 ± 2185	−51 ± 4	−6 ± 1	33 ± 6
Tongue, Right				
First	3042 ± 1640	56 ± 2	−6 ± 3	28 ± 5
Second	2589 ± 2121	56 ± 4	−7 ± 4	31 ± 6

Note.—COGs are the Talairach coordinates. Data are from the single-subject analysis. Numbers of subjects were as follows: 12 for the hand, fingers, wrist, and elbow experiments and 11 for the tongue and foot experiments.

significant differences in the geometric centers indicate a clear fine-scale somatotopic gradient for the wrist, elbow, fingers, and hand, despite the considerable overlap of the activated volumes (3). The high degree of reproducibility of the COG locations, both within and across subjects, is attributed to the well-standardized experimental conditions and the use of a custom-designed device to control the movements (4). Methodologically, the volumes of activation were unreliable parameters, because they had a large intra- and intersubject variability, in contrast to the COGs.

Topographic Organization of the Primary Motor Cortex

Early experimental data in a variety of mammals have suggested that body representation in M1 is apparent in somatotopically organized maps in which muscles, joints, and body parts are localized in an orderly manner (30). This global scheme implies that circumscribed parts of M1 are devoted to the control of specific muscle groups. Although the large-scale somatotopy within M1 is no longer questioned, the topographic organization of the within-forelimb representation has triggered many investigations in nonhuman primates and in humans. In their original study, Penfield and Boldrey (3) had already shown that the within-forearm representation was not as simple as the iconic maps suggest and that movements of elbow, wrist, and (specifically) fingers could be evoked from widely distributed stimulation points scattered through the entire M1 area for the arm.

Since the time of these classic studies, work in monkeys has provided a body of experimental evidence. Based on intracortical microstimulation and receptive field properties, the results suggest that alternative organizational principles underlying the M1 hand area exist. According to Strick and Preston (31), a double representation of hand and fingers is present in the monkey. This observation is supported by in recent findings from cytoarchitectonic, neurotransmitter, and neuroimaging studies in humans that reveal anterior (4a) and posterior (4p) M1 finger representation with different functional specializations (15, 28). In the monkey, another scheme proposed by Kwan et al (32) and confirmed in several studies (33, 34) described the topographic organization of the M1 forelimb region as a horseshoe-shaped or nested structure in which the fingers are in the core and surrounded by the wrist, then the elbow, and finally the shoulder. Some have suggested that such topography within the arm representation functions to smoothly and promptly organize the muscle synergies required in most movements. Finally, with respect to the fingers, Schieber and Hibbard (7) elegantly demonstrated in monkeys that each finger is controlled by widely overlapping populations of neurons in the M1 finger region.

Functional Neuroimaging Studies in Humans

Neuroimaging findings in humans also support the presence of multiple activation sites for individual finger movements (8), and the support the lack of a clear somatotopy for different fingers (9). However, a method involving contrasting finger movements as the control task revealed an orderly topographic progression in the hand area, with the thumb area located most laterally (10). This last finding was recently supported by results of fMR imaging studies that mainly focused on finger representation (29, 35, 36).

The results of our study are in line with several previous observations showing isolated, gross subdivisions for the foot, arm, and face areas (12, 14, 37). In addition, the results also indicate a complex organization in the M1 arm region, with considerable overlap of the activated volumes. These findings can be extended to the descriptions of wrist and elbow representations in the previous reports. Furthermore, our quantitative assessment based on COGs revealed a notable somatotopic progression in the forearm representation; this finding corresponds to the scheme proposed by Penfield and supports other observations (11, 29, 35, 36, 38). The use of COGs is a powerful method for analyzing the cortical representation of distinct body parts, and it also allows a comparison of our findings with those of other imaging studies. The COGs obtained for the sequential finger to thumb opposition (x, −37; y, −20; z, 58) in the present study were similar to the statistical maxima reported with positron emission tomography (PET) (11, 15, 38) and fMR imaging (14) (Table 1). Because of methodological constraints (transformation into the Talairach space and blurring of the functional data), neither the horseshoe nor a poten-

tial double-hand representation could be investigated in this study.

Standardization and Reproducibility

The results from a single fMR imaging session were typically indicative of the subject's functional neuroanatomy. Underlying this interpretation is the implicit assumption that we had no biased responses that were specific to a particular session. That is, the potential variability of responses between sessions was negligible. However, the results of an individual imaging session is only one distinct representation of a subject's brain function at a specific point in time, and it may not delineate all of the reactions to a specific sensorimotor challenge (16). Furthermore, differences between sessions are inevitable. For example, the BOLD response is an indirect and semiquantitative measure of neuronal activity, and a number of physiologic factors influence the relationship between BOLD contrast and cerebral oxygen metabolism (39). Also, slight variations in the hardware characteristics of the MR machine that are not systematic across sessions (eg, shim performed to homogenize the B_0 field of the scanner) may influence the single-session results (16). In addition, nonspecific physiologic effects, such as the level of arousal and attention, can further influence the neurovascular response elicited by the specific activation task (40). All of these possibilities may account for the considerable intra- and interindividual variations in the volumes of activation that we and other investigators observed despite the well-controlled conditions. In fact, attempts to examine the test-retest reliability of fMR imaging by using measures such as voxel counting on thresholded maps are limited by an arbitrarily defined statistical threshold and by the loss of complexity that accompanies a method in which voxels are classified as being either active or inactive (16).

Functional imaging studies of the reproducibility and consistency in the human motor system are rare (11, 13, 15, 16). This lack is an important shortcoming in view of the high interindividual variability of the COGs for various movements, as were reported in a recent fMR imaging study and attributed to individual variations in movement execution (14). To our knowledge, no single study has been devoted to assessing the reproducibility of the somatotopic organization of M1. Three groups have addressed the issue of reproducibility in fMR imaging, but only for finger movements. In a single subject, Wexler et al (13) demonstrated consistent and localized activation in the contralateral M1 finger region over nine sessions. Carey et al (15) used a mechanical support for the hand and forearm, as we did, and found a high degree of consistency in the finger representation between PET imaging sessions. McGonigle et al (16) repeated a finger tapping experiment 33 times in one single subject to determine how well a single individual typified the subjects response across multiple sessions. They found substantial session-by-condition interactions in each of the multisession data sets. This result illustrates the influence of session context on the results of any individual experiment and shows the potential danger of drawing general conclusions from an individual session. Our findings demonstrate a high degree of reliability in the large-scale, and particularly the fine-scale, somatotopy both within and across subjects. Highly consistent COGs with low SDs and only negligible variations in location were found. The standardization of the movements is most likely responsible for these findings, although no specific comparison with uncontrolled conditions was performed. The residual variations of a few millimeters are in the range of the methodological accuracy inherent to volume registration into Talairach space. Potential inaccuracies due to echo-planar distortions could be ruled out by means of visual inspection so that no substantial distortion could be observed in the vertex regions. On echo-planar images, distortions in other regions (cranial base, next to the sinuses, occipital lobes) did not impair the registration to Talairach space that we performed with the undistorted conventional images.

All together, these results demonstrate that, in addition to global factors affecting the activation state of the whole brain (40), the performance of controlled movements can improve the reproducibility of the fMR imaging data.

Conclusion

Our results confirm a refined concept of the M1 topographic organization that consists of a large-scale somatotopy with distinct regions for separate body parts and a complex fine-scale organization for intralimb representations. The results further demonstrate high intra- and interindividual consistency in the geometric locations of activation clusters when controlled and standardized experimental conditions are applied. In extending motor studies to patient populations, knowledge of the expected variations in matched healthy volunteers is essential to interpret the changes observed in individual patients. Moreover, the reproducibility of brain activation patterns over time is crucial for monitoring functional reorganization, particularly in follow-up studies during rehabilitation after surgical intervention or cerebral infarct occurs.

References

1. Hughlings Jackson J **Convulsive spasms of the right hand and arm preceding epileptic seizures.** *Med Times Gaz* 1863;1:589
2. Foerster O. **Motorische Felder und Bahnen.** In: Bumke H, Foerster O, eds. *Handbuch der Neurologie IV.* Berlin: Springer-Verlag; 1936; 49–56
3. Penfield W, Boldrey E. **Somatic motor and sensory representation in the cerebral cortex of man as studies by electrical stimulation.** *Brain* 1937;60:389–443
4. Hepp-Reymond MC. **Functional organization of motor cortex and its participation in voluntary movements.** In: Setklis HD, Erwin J, eds. *Comparative Primate Biology Volume 4: Neurosciences,* New York: Alan R. Liss, Inc; 1988:501–624
5. Lemon R. **Mapping the output functions of the motor cortex.** In: Edelman G, Gall W, Cowan W, eds. *Signal and Sense* New York: Wiley-Liss; 1990:315–355

6. Donoghue JP, Leibovic S, Sanes JN. **Organization of the forelimb area in squirrel monkey motor cortex: representation of digit, wrist, and elbow muscles.** *Exp Brain Res* 1992;89:1–19
7. Schieber MH, Hibbard LS. **How somatotopic is the motor cortex hand area?** *Science* 1993;261:489–492
8. Sanes JN, Donoghue JP, Thangaraj V, Edelman RR, Warach S. **Shared neural substrates controlling hand movements in human motor cortex.** *Science* 1995;268:1775–1777
9. Volkmann J, Schnitzler A, Witte O, Freund H. **Handedness and asymmetry of hand representation in human motor cortex.** *J Neurophysiol* 1998;79:2149–2154
10. Kleinschmidt A, Nitschke MF, Frahm J. **Somatotopy in the human motor cortex hand area: a high-resolution functional MRI study.** *Eur J Neurosci* 1997;9:2178–2186
11. Grafton ST, Woods RP, Mazziotta JC. **Within-arm somatotopy in human motor areas determined by positron emission tomography imaging of cerebral blood flow.** *Exp Brain Res* 1993;95:172–176
12. Fink GR, Frackowiak RS, Pietrzyk U, Passingham RE. **Multiple nonprimary motor areas in the human cortex.** *J Neurophysiol* 1997; 77:2164–2174
13. Wexler BE, Fulbright RK, Lacadie CM, et al. **An fMRI study of the human cortical motor system response to increasing functional demands.** *Magn Reson Imaging* 1997;15:385–396
14. Lotze M, Erb M, Flor H, Huelsmann E, Godde B, Grodd W. **FMRI evaluation of somatotopic representation in human primary motor cortex.** *Neuroimage* 2000;11:473–481
15. Carey LM, Abbott DF, Egan GF, Tochon-Danguy HJ, Donnan GA. **The functional neuroanatomy and long-term reproducibility of brain activation associated with a simple finger tapping task in older healthy volunteers: a serial PET study.** *Neuroimage* 2000;11:124–144
16. McGonigle DJ, Howseman AM, Athwal BS, Friston KJ, Frackowiak RSJ, Holmes AP. **Variability in fMRI: An examination of intersession differences.** *Neuroimage* 2001;11:708–734
17. Chapman LJ, Chapman JP. **The measurement of handedness.** *Brain Cogn* 1987;6:175–183
18. Alkadhi H, Kollias SS, Crelier GR, Golay X, Hepp-Reymond MC, Valavanis A. **Plasticity of the human motor cortex in patients with arteriovenous malformations: an fMRI study.** *AJNR Am J Neuroradiol* 2000;21:1423–1433
19. Dai TH, Liu JZ, Sahgal V, Brown RW, Yue GH. **Relationship between muscle output and functional MRI-measured brain activation.** *Exp Brain Res* 2001;140:290–300
20. Woods RP, Grafton ST, Holmes CJ, Cherry SR, Mazziotta JC. **Automated image registration, I: General methods and intrasubject, intramodality validation.** *J Comput Assist Tomogr* 1998;22:139–152
21. Hopfinger JB, Buchel C, Holmes AP, Friston KJ. **A study of analysis parameters that influence the sensitivity of event-related fMRI analyses.** *Neuroimage* 2000;11:326–333
22. Collins DL, Neelin P, Peters TM, Evans AC. **Automatic 3D intersubject registration of MR volumetric data in standardized Talairach space.** *J Comput Assist Tomogr* 1994;18:192–205
23. Bandettini PA, Jesmanowica A, Wong EC, Hyde JS. **Processing strategies for time-course data sets in functional MRI of the human brain.** *Magn Reson Med* 1993;30:161–173
24. Press WH. **Nonparametric or rank correlation.** In: Press WH, Teukolsky SA, Vetterling WT, Flannery BP, eds. *Numerical Recipes in C: The Art of Scientific Computing.* New York: Cambridge University Press; 1992:639–644
25. Worsley KJ, Marrett S, Neelin P, Vandal AC, Friston KJ, Evans AC. **A unified statistical approach for determining significant signals in images of cerebral activation.** *Human Brain Mapping* 1996;4:58–73
26. Glover GH. **Deconvolution of impulse response in event-related BOLD fMRI.** *Neuroimage* 1999;9:416–429
27. Kiebel SJ, Poline JB, Friston KJ, Holmes AP, Worsley KJ. **Robust smoothness estimation in statistical parametric maps using standardized residuals from the general linear model.** *Neuroimage* 1999;10:756–766
28. Geyer S, Ledberg A, Schleicher A, et al. **Two different areas within the primary motor cortex of man.** *Nature* 1996;382:805–807
29. Beisteiner R, Windischberger C, Lanzenberger R, et al. **Finger somatotopy in human motor cortex.** *Neuroimage* 2001;13:1016–1026
30. Woolsey CN, Settlage PH, Meyer DR, Sencer W, Hamuy TP, Travis AM. **Patterns of localization in precentral and "supplementary" motor areas and their relation to the concept of a premotor area.** *Res Publ Assoc Res Nerv Ment Dis* 1952;30:238–264
31. Strick PL, Preston JB. **Two representations of the hand in area 4 of a primate, I: motor output organization.** *J Neurophysiol* 1982;48: 139–149
32. Kwan HC, MacKay WA, Murphy JT, Wong YC. **Spatial organization of precentral cortex in awake primates, II: motor outputs.** *J Neurophysiol* 1978;41:1120–1131
33. Sessle BJ, Wiesendanger M. **Structural and functional definition of the motor cortex in the monkey (Macaca fascicularis).** *J Physiol Lond* 1982;323:245–65
34. Wannier TM, Maier MA, Hepp-Reymond MC. **Contrasting properties of monkey somatosensory and motor cortex neurons activated during the control of force in precision grip.** *J Neurophysiol* 1991;65:572–589
35. Indovina I, Sanes JN. **On somatotopic representation centers for finger movements in human primary motor cortex and supplementary motor area.** *Neuroimage* 2001;13:1027–1034
36. Hlustik P, Solodkin A, Gullapalli RP, Noll DC, Small SL. **Somatotopy in human primary motor and somatosensory hand representations revisited.** *Cerebral Cortex* 2001;11:312–321
37. Rao SM, Binder JR, Hammeke TA, et al. **Somatotopic mapping of the human primary motor cortex with functional magnetic resonance imaging.** *Neurology* 1995;45:919–924
38. Colebatch JG, Deiber MP, Passingham RE, Friston KJ, Frackowiak RS. **Regional cerebral blood flow during voluntary arm and hand movements in human subjects.** *J Neurophysiol* 1991;65:1392–1401
39. Ogawa S, Menon RS, Kim SG, Ugurbil K. **On the characteristics of functional magnetic resonance imaging of the brain.** *Annu Rev Biophys Biomol Struct* 1998;27:447–474
40. Waldvogel D, Van Gelderen P, Immisch L, Pfeiffer C, Hallett M. **The variability of serial fMRI data: correlation between a visual and a motor task.** *Neuroreport* 2000;27:3843–3847